YTHDF3 modulates hematopoietic stem cells by recognizing RNA m^{6}A modification on *Ccnd1*

Xiaofei Zhang,[1*] Tingting Cong,[1*] Lei Wei,[2] Bixi Zhong,[2] Xiaowo Wang,[2] Jin Sun,[3] Shuxia Wang,[3] Meng Michelle Xu,[4] Ping Zhu,[3] Hong Jiang[5] and Jianwei Wang[1]

[1]School of Pharmaceutical Sciences, Tsinghua University, Beijing; [2]Ministry of Education Key Laboratory of Bioinformatics, Center for Synthetic and Systems Biology, Bioinformatics Division, BNRIST, Department of Automation, Tsinghua University, Beijing; [3]Department of Geriatrics, The Second Medical Center & National Clinical Research Center for Geriatric Diseases, Chinese PLA General Hospital, Beijing; [4]Department of Basic Medical Sciences, School of Medicine, Institute for Immunology, Beijing Key Lab for Immunological Research on Chronic Diseases, THU-PKU Center for Life Sciences, Tsinghua University, Beijing and [5]Kidney Disease Center, the First Affiliated Hospital, College of Medicine, Zhejiang University, Hangzhou, China

**XZ and TC contributed equally as co-first authors.*

Correspondence:
Ping Zhu
zhuping301hospital@163.com
Hong Jiang
jianghong961106@zju.edu.cn
Jianwei Wang
jianweiwang@mail.tsinghua.edu.cn

Received: July 30, 2021.
Accepted: November 25, 2021.
Prepublished: February 3, 2022.

https://doi.org/10.3324/haematol.2021.279739

Abstract

Hematopoietic stem cells (HSC) give rise to the cells of the blood system over the whole lifespan. N6-methyladenosine (m^{6}A), the most prevalent RNA modification, modulates gene expression via the processes of "writing" and "reading". Recent studies showed that m^{6}A "writer" genes (*Mettl3* and *Mettl14*) play an essential role in HSC. However, which reader deciphers the m^{6}A modification to modulate HSC remains unknown. In this study, we observed that dysfunction of *Ythdf3* and *Ccnd1* severely impaired the reconstitution capacity of HSC, which phenocopies *Mettl3*-deficient HSC. Dysfunction of *Ythdf3* and *Mettl3* results in a translational defect of *Ccnd1*. *Ythdf3* and *Mettl3* regulate HSC by transmitting m^{6}A RNA methylation on the 5' untranslated region of *Ccnd1*. Enforced *Ccnd1* expression completely rescued the defect of *Ythdf3*$^{-/-}$ HSC and partially rescued *Mettl3*-compromised HSC. Taken together, this study identified, for the first time, that *Ccnd1* is the target of METTL3 and YTHDF3 to transmit the m^{6}A RNA methylation signal and thereby regulate the reconstitution capacity of HSC.

Introduction

Hematopoietic stem cells (HSC) generate all blood cells and themselves throughout life, a function that is achieved through differentiation and self-renewal.[1,2] Therefore, discovering the molecular mechanisms modulating HSC differentiation and self-renewal is of great importance to understand the nature of the blood system and hematopoietic malignancies. Although some studies have revealed several molecular mechanisms regulating HSC,[3] the exact mechanisms are still not fully understood. In recent years, post-transcriptional chemical modifications, which are introduced at specific sites of RNA, have become an emerging field of interest.[4] Among the various RNA alterations, N6-methyladenosine (m^{6}A) is the most abundant nucleotide modification in messenger RNA (mRNA), which functions through the processes of "writing", "erasing" and "reading".[5] A few genes are responsible for the process of "writing" the m^{6}A code, including *Mettl3*, *Mettl14*, *Wtap*, *Zc3h13*, *Kiaa1429*, *Rbm15* and *Rbm15b*,[6-8] with Mettl3 being the catalytic core;[6,9] m^{6}A methylation can be reversed via active demethylation by m^{6}A demethylases FTO or ALKBH5. YTH domain-carrying genes, including *Ythdf1*, *Ythdf2* and *Ythdf3*,[10] are responsible for the process of "reading" the m^{6}A code by selectively binding to m^{6}A-containing transcripts and have the function of modifying m^{6}A.[10-13] *Ythdf1* regulates the translation efficiency by binding m^{6}A-modified mRNA,[13] *Ythdf2* decreases mRNA stability by recruiting the CCR4-NOT deadenylase complex,[12,14] and *Ythdf3* facilitates translation or decay of m^{6}A-modified mRNA through cooperation with *Ythdf1* or *Ythdf2*.[11,15]

Yao *et al.* reported that in the hematopoietic system, the METTL3 and METTL14 complex regulates the self-renewal capacity of HSC.[16] Two more studies documented that Mettl3 modulates the differentiation and symmetric commitment of HSC by targeting *Myc*.[17,18] Given that m^{6}A methylation exerts its effects through reader proteins, and that RNA m^{6}A modification participates in diverse eukaryotic biological processes[19-20] and tumor initi-

ation,[21,22] elucidating the function of m^{6}A reader proteins will probably be crucial to uncovering the biological significance of the m^{6}A modification. Two recent studies have shown that loss of *Ythdf2* promotes HSC expansion and regeneration,[23,24] which is completely different from the phenotype of *Mettl3* or *Mettl14* dysfunctional HSC in which loss of these genes severely impairs HSC function.[16-18] It would, therefore, be intriguing to know on which gene(s) METTL3 writes the m^{6}A signal and which reader recognizes this modification to regulate HSC function.

In this study, we observed that dysfunction of *Ythdf3*, but not of *Ythdf1*, impairs the reconstitution capacity of HSC, recapitulating the phenotype of *Mettl3* dysfunctional HSC. The 5'-untranslated region (UTR) of *Ccnd1* is the hub of METTL3 and YTHDF3 to transmit the m^{6}A signal to regulate the translation of *Ccnd1*, and furthermore to modulate the reconstitution capacity of HSC. Enforced *Ccnd1* expression completely rescued the functional defect of *Ythdf3*$^{-/-}$ HSC, and partially rescued *Mettl3*-compromised HSC. Ectopic MYC only rescued the differentiation skewing of *Mettl3*-compromised HSC, but not the reconstitution capacity. Taken together, our study reveals, for the first time, that *Ythdf3* deciphers the m^{6}A modification on *Ccnd1* to modulate HSC, and provides a reference for how the RNA m^{6}A modification regulates stem cell function.

Methods

Mice

Mettl3$^{fl/fl}$, *Ythdf1*$^{-/-}$ and *Ythdf3*$^{-/-}$ mice were generated in Cyagen Biosciences Inc. (Guangzhou, China). All mice were kept in specific pathogen-free conditions and all procedures were approved by the Institutional Animal Care and Use Committee of Tsinghua University. Full details are supplied in the *Online Supplementary Methods*.

Results

Dysfunction of *Ythdf3*, but not *Ythdf1*, mildly disturbs the hematopoietic system

Given that m^{6}A reader proteins are responsible for exerting the action of m^{6}A, and that *Ythdf2*-deficient HSC exhibit increased self-renewal capacity,[23,24] which is not consistent with the phenotype of *Mettl3*$^{-/-}$ HSC,[16-18] we generated *Ythdf1* and *Ythdf3* knockout mice to investigate the function of these two m^{6}A readers in HSC (Figure 1A, B). Both strains of mice develop normally and can reproduce. Complete blood counts, including white blood cell, lymphocyte, neutrophil, red blood cell and platelet counts, revealed no difference between *Ythdf1*$^{-/-}$, *Ythdf3*$^{-/-}$ and control mice (Figure 1C, D). In addition, the bone marrow cellularity of *Ythdf1*$^{-/-}$ and *Ythdf3*$^{-/-}$ was indistinguishable from that of control mice (*Online Supplementary Figure S1A-D*). We then sought to investigate the lineage composition, including T, B and myeloid cells, in peripheral blood and bone marrow of *Ythdf1*$^{-/-}$ and *Ythdf3*$^{-/-}$ mice. The results revealed no difference between *Ythdf1*$^{-/-}$ and WT mice in either the peripheral blood (Figure 1E) or the bone marrow (*Online Supplementary Figure S1G*). As for *Ythdf3*$^{-/-}$ mice, the percentages of B and myeloid cells remained stable in peripheral blood and bone marrow compared to those in WT mice (Figure 1F and *Online Supplementary Figure S1H*), while the percentages of CD4$^+$ and CD8$^+$ T cells decreased slightly in bone marrow (1.58±0.24 *vs*. 1.11±0.14, 1.62±0.26 *vs*. 1.15±0.14), but not in peripheral blood (10.94±1.50 *vs*. 10.54±1.65, 12.52±0.99 *vs*. 12.95±0.78) (Figure 1F and *Online Supplementary Figure S1H*). We then compared the frequencies of T cells in spleen and thymus between *Ythdf3*$^{-/-}$ and WT mice, without finding a significant difference (*Online Supplementary Figure S1I, J*).

We next analyzed hematopoietic stem and progenitor cells of *Ythdf1*$^{-/-}$ and *Ythdf3*$^{-/-}$ mice, including common myeloid progenitors, granulocyte-macrophage progenitors, megakaryocyte-erythroid progenitors, common lymphoid progenitors, multipotent progenitor cells and HSC. We observed that the frequencies and absolute numbers of these cells remained the same between *Ythdf1*$^{-/-}$ and WT mice (Figure 1G, H and *Online Supplementary Figure S1B, C*). Likewise, the frequencies and absolute numbers of common myeloid, granulocyte-macrophage, megakaryocyte-erythroid, and common lymphoid progenitors, as well as multipotent progenitor cells in *Ythdf3*$^{-/-}$ mice were comparable with those in WT mice (Figure 1I and *Online Supplementary Figure S1E*). However, the frequency and absolute number of *Ythdf3*$^{-/-}$ HSC were iincreased significantly (64.31±10.34 *vs*. 106.01±6.99, 1.90±0.31 *vs*. 2.82 *vs*. 0.23) (Figure 1J and *Online Supplementary Figure S1F*), resembling those of *Mettl3*$^{-/-}$ mice.[16,17] Cell cycle analysis revealed no difference between *Ythdf3*$^{-/-}$ and WT HSC (*Online Supplementary Figure S1K, L*).

The reconstitution capacity of *Ythdf3*-deficient hematopoietic stem cells is impaired

To further investigate the reconstitution capacity of *Ythdf1*$^{-/-}$ and *Ythdf3*$^{-/-}$ HSC, 25 freshly isolated *Ythdf1*$^{-/-}$, *Ythdf3*$^{-/-}$ and WT HSC were transplanted into lethally irradiated recipients together with 2.5×10^5 competitor cells (Figure 2A). We observed no obvious differences of peripheral blood chimera and lineage distribution between *Ythdf1*$^{-/-}$ and WT HSC (Figure 2B and *Online Supplementary Figure S2A*). By contrast, the reconstitution capacity of *Ythdf3*$^{-/-}$ HSC was severely impaired (71.63±4.66 *vs*. 29.03±10.82 at the fourth month), including B, T and myeloid lineages (Figure 2C). The lineage distribution exhibited

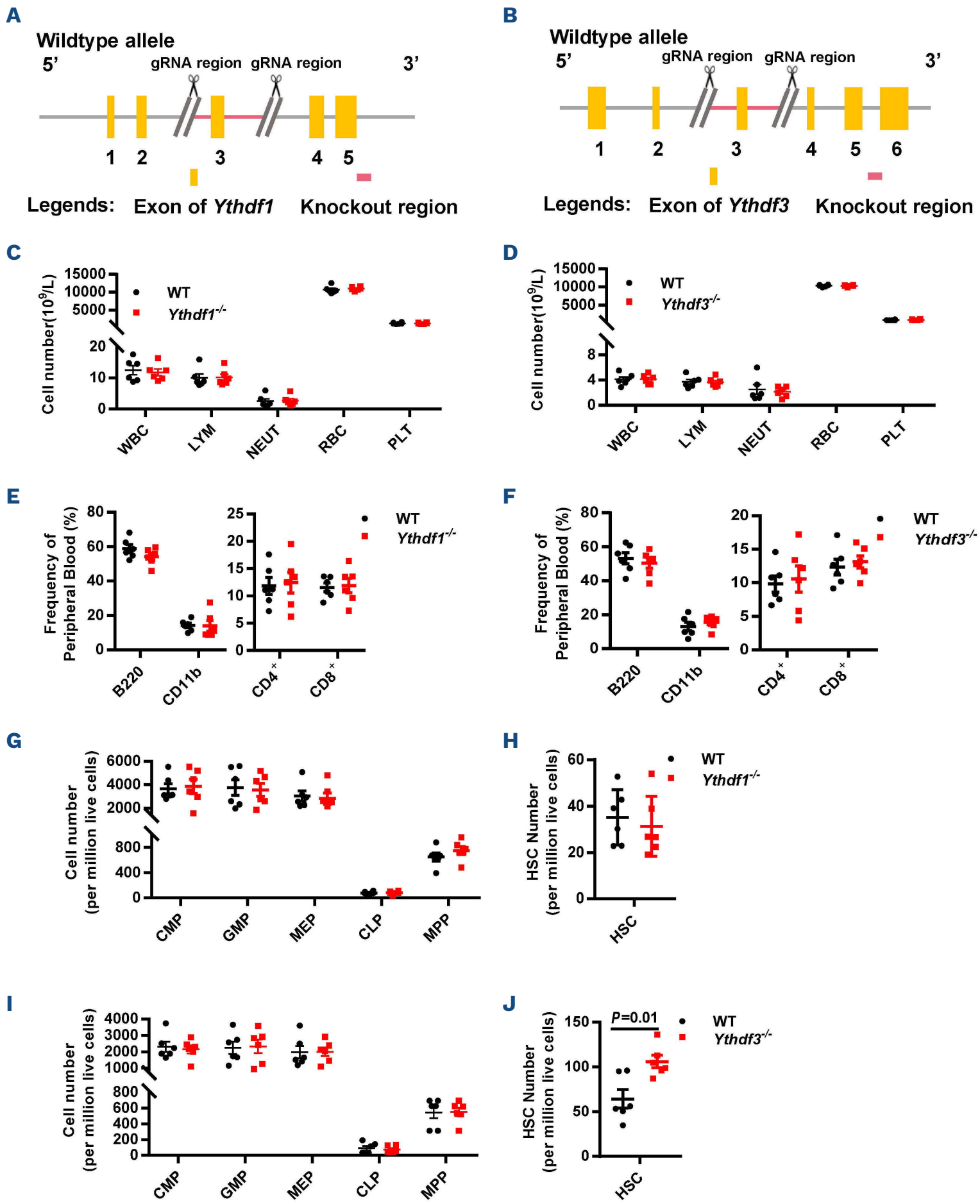

Figure 1. Dysfunction of *Ythdf3*, but not *Ythdf1*, mildly disturbs the hematopoietic system. (A) Diagram of the production of *Ythdf1* knockout mice. (B) Diagram of the production of *Ythdf3* knockout mice. (C, D) The scatter plots show the differences in counts of white blood cells, lymphocytes, neutrophils, red blood cells and platelets between wildtype (WT) and *Ythdf1*$^{-/-}$ mice (C), as well as WT and *Ythdf3*$^{-/-}$ mice (D) (2 months old) as determined by an automatic peripheral blood analyzer. Six mice per group. Data are shown as mean ± standard error of mean (SEM). (E, F) The scatter plots depict the percentages of myeloid, B and T cells in peripheral blood for WT and *Ythdf1*$^{-/-}$ mice (E), as well as for WT and *Ythdf3*$^{-/-}$ mice (F) (2 months old). Six mice per group. Data are shown as mean ± SEM. (G-J) The scatter plots depict the numbers of common myeloid progenitors, granulocyte-macrophage progenitors, megakaryocyte-erythroid progenitors, common lymphoid progenitors, and multipotent progenitor cells per 10^6 bone marrow cells in WT and *Ythdf1*$^{-/-}$ mice (G), as well as in WT and *Ythdf3*$^{-/-}$ mice (I) (2 months old), and the number of hematopoietic stem cells per 10^6 bone marrow cells in WT and *Ythdf1*$^{-/-}$ mice (H), and WT and *Ythdf3*$^{-/-}$ mice (J) (2 months old). Six mice per group. Data are shown as mean ± SEM. WBC: white blood cells; LYM: lymphocytes; NEUT: neutrophils; RBC: red blood cells; PLT: platelets; CMP: common myeloid progenitors; GMP: granulocyte-macrophage progenitors; MEP: megakaryocyte-erythroid progenitors; CLP: common lymphoid progenitors; MPP: multipotent progenitor cells; HSC: hematopoietic stem cells.

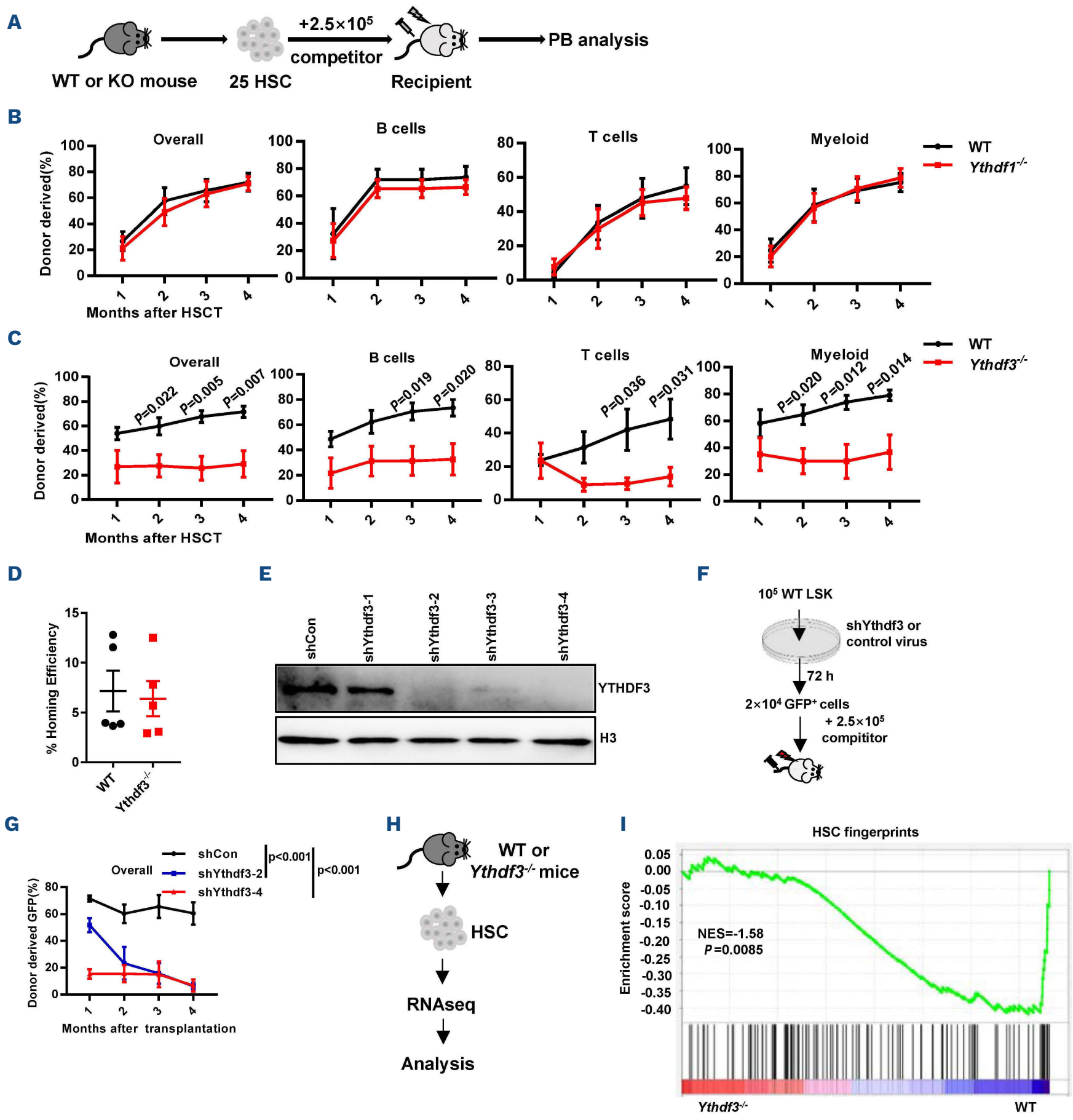

Figure 2. The reconstitution capacity of *Ythdf3*-deficient hematopoietic stem cells is impaired. (A) Scheme of the competitive transplantation strategy for *Ythdf1*$^{-/-}$ and *Ythdf3*$^{-/-}$ hematopoietic stem cells (HSC). (B, C) Freshly isolated HSC (n=25) from 2-month-old knockout mice or wildtype (WT) mice were transplanted into lethally irradiated recipients together with 2.5×10^5 competitor cells. Engraftment of donor cells was determined in overall (CD45.2$^+$), myeloid (Mac-1$^+$), B (B220$^+$) and T (CD3$^+$) cells every month after transplantation. The line plots depict the percentages of donor-derived cells (overall, B cells, myeloid cells, T cells) in recipient WT and *Ythdf1*$^{-/-}$ mice (B), and WT and *Ythdf3*$^{-/-}$ mice (C) at the indicated time points. Five mice per group. Data are shown as mean ± standard error of mean (SEM). (D) The scatter plots show the percentage of *Ythdf3*$^{-/-}$ Lin$^-$ Sca1$^+$ cells that homed to the bone marrow relative to control. Five mice per group. Data are shown as mean ± SEM. (E) Freshly isolated LSK cells were infected by lentivirus carrying *Ythdf3* shRNA or control shRNA; 4 days later, 10^5 GFP$^+$ cells were purified for western blot to evaluate the expression of YTHDF3. (F, G) Freshly isolated WT LSK cells were infected by lentivirus carrying *Ythdf3* shRNA or control; 72 h later, 20,000 GFP$^+$ cells were purified and transplanted into lethally irradiated recipients together with 2.5×10^5 competitor cells. Chimerism in peripheral blood was evaluated every month until the fourth month. (F) Experimental design to evaluate the reconstitution capacity of *Ythdf3* shRNA-carrying HSC. (G) Line plots depicting the percentages of GFP$^+$ cells in donor-derived cells every month after transplantation. Six or seven mice per group. Data are shown as mean ± SEM. (H) Experimental design of the RNA-sequencing assay (see Methods). (I) These figures show the gene set enrichment analysis of HSC fingerprint genes in *Ythdf3*$^{-/-}$ HSC *versus* WT HSC. The normalized enrichment score is |>0.3; *P*<0.05 represents a statistically significant difference. KO: knockout; PB: peripheral blood; HSCT: hematopoietic stem cell transplantation; NES: normalized expression score.

no obvious differentiation bias between *Ythdf3*$^{-/-}$ and WT mice (*Online Supplementary Figure S2B*). We also counted the donor-derived HSC in the bone marrow of recipients at the end of the fourth month after transplantation and found no significant difference between *Ythdf3*$^{-/-}$ and WT recipients (*Online Supplementary Figure S2C, D*).

In order to rule out the possibility that the impaired reconstitution capacity of *Ythdf3*$^{-/-}$ HSC was due to impaired homing capacity, we performed short-term homing assays for *Ythdf3*$^{-/-}$ and WT HSC according to standard protocols.[25,26] The results showed no significant difference in homing efficiency between *Ythdf3*$^{-/-}$ and WT Lin$^-$ Sca1$^+$ cells (Figure 2D).

To rule out the possibility that *Ythdf3* is compensated for during the embryonic stage of *Ythdf3*$^{-/-}$ mice, we generated two efficient short hairpin RNA (shRNA) against *Ythdf3*: *shYthdf3-2* and *shYthdf3-4* (Figure 2E). Freshly isolated WT LSK cells (Lin$^-$ Sca1$^+$ cKit$^+$) were infected by *Ythdf3* shRNA-carrying lentivirus. Seventy-two hours later, 20,000 green fluorescent protein (GFP)$^+$ cells were purified and transplanted into lethally irradiated recipients together with 2.5×10^5 competitor cells (Figure 2F). The results showed that the reconstitution capacity of *Ythdf3* shRNA-carrying cells was severely impaired (shRNA-2: 6.13±2.82 *vs*. 60.51±8.33; shRNA-4: 6.74±4.55 *vs*. 60.51±8.33 at the fourth month), including the rconstitituion of B, T and myeloid lineages (Figure 2G and *Online Supplementary Figure S2E*). To further investigate the transcriptional difference between *Ythdf3*$^{-/-}$ and WT HSC, we performed RNA sequencing for those cells (Figure 2H). With principal component analysis, we found that the expression patterns of the *Ythdf3*$^{-/-}$ HSC were distinct from those of WT ones (*Online Supplementary Figure S2F*). Gene set enrichment analysis (GSEA) revealed that the HSC fingerprint genes were no longer enriched among *Ythdf3*$^{-/-}$ HSC (Figure 2I), coinciding with the impaired reconstitution capacity of *Ythdf3*$^{-/-}$ HSC. Furthermore, we analyzed apoptosis-related genes between *Ythdf3*$^{-/-}$ and WT HSC by GSEA, and found no significant difference (*Online Supplementary Figure S2G*). We then wondered whether *Ythdf3*$^{-/-}$ HSC undergo cell death during *in vitro* culture. Freshly isolated LSK cells from *Ythdf3*$^{-/-}$ and WT mice were cultured in serum-free expansion medium with the cytokines, stem cell factor and thrombopoietin. The percentage of annexin V-positive cells was analyzed 24 h later (*Online Supplementary Figure S2H*) and found to be significantly increased in *Ythdf3*$^{-/-}$ LSK cells (*Online Supplementary Figure S2I,J*). This result indicates that *Ythdf3*$^{-/-}$ hematopoietic stem and progenitor cells are more sensitive to replication stress.

Given that ribosomes are the site of protein synthesis, we then evaluated protein synthesis-related signaling and observed that ribosome pathway and ribosome-related genes were downregulated in *Ythdf3*$^{-/-}$ HSC (*Online Supplementary Figure S3A, B*). To further investigate this, we sought to measure protein synthesis in *Ythdf3*$^{-/-}$ LSK cells. In this assay, LSK cells were incubated with a puromycin analog (OPP), which is incorporated into nascent polypeptide chains and then fluorescently labeled via a "click reaction". The results showed that the protein synthesis of *Ythdf3*$^{-/-}$ LSK cells was significantly decreased (*Online Supplementary Figure S3C-E*). Briefly, these data provide the confirmation that *Ythdf3*, but not *Ythdf1*, modulates the reconstitution capacity of HSC.

YTHDF3, but not YTHDF1, modulates the translation of CCND1

Our data indicate that the reconstitution capacity of *Ythdf3*$^{-/-}$ HSC resembles that of *Mettl3*$^{-/-}$ HSC,[16,17] and a previous study revealed that *Ythdf3* plays a critical role in translating m^{6}A-modified mRNA.[11] Moreover, two recent studies found that *Ythdf2*$^{-/-}$ HSC exhibit enhanced reconstitution capacity[23,24] and *Ythdf3* shares targets with *Ythdf2*.[11] We speculated that *Ythdf3* may modulate the targets of *Ythdf2* oppositely to regulate the function of HSC. We therefore investigated the six genes (*MYC*, *CCND1*, *AXIN2*, *MCL-1*, *CD133* and *BCL2*) which were significantly increased in *Ythdf2*$^{-/-}$ HSC,[23] determining their expression in *Ythdf3*$^{-/-}$ LSK cells by western blotting assays. The assays showed that only *CCND1* was decreased, while *MYC*, *MCL-1*, *CD133*, *AXIN2* and *BCL2* remained stable compared to those in the controls (Figure 3A). Moreover, we found that knockout of *Ythdf3* did not affect the mRNA expression level of *Ccnd1* in LSK cells (Figure 3B).

To further confirm this observation, we infected WT LSK cells by lentivirus carrying shRNA against *Ythdf3* to evaluate the expression of *Ccnd1* (Figure 3C). Knockdown of *Ythdf3* significantly reduced the protein level of CCND1 (Figure 3D), but not the mRNA level (Figure 3E). A previous study showed that YTHDF3 promotes protein synthesis in synergy with YTHDF1,[11] so we wondered whether YTHDF1 is involved in CCND1 translation. We evaluated the protein expression of CCND1 in *Ythdf1*$^{-/-}$ LSK cells and found no difference of CCND1 between *Ythdf1*$^{-/-}$ and WT LSK cells (*Online Supplementary Figure S4A*), indicating that YTHDF3 modulates the translation of *Ccnd1* via a YTHDF1-independent manner. In brief, the above data suggest that *Ythdf3*, but not *Ythdf1*, regulates *Ccnd1* through post-transcriptional modification.

YTHDF3 promotes the translation of CCND1 by binding to the 5' untranslated region

A previous study revealed that FTO demethylates m^{6}A-modified *Ccnd1* mRNA[27] and our results indicated that Ccnd1 is regulated post-transcriptionally by *Ythdf3* (Figure 3A-E). We were tempted to speculate that *Ccnd1* may be regulated by YTHDF3 through m^{6}A modification. To test our hypothesis, we predicted the putative m^{6}A motif on *Ccnd1* by using SRAMP.[28] *In silico* analysis predicted

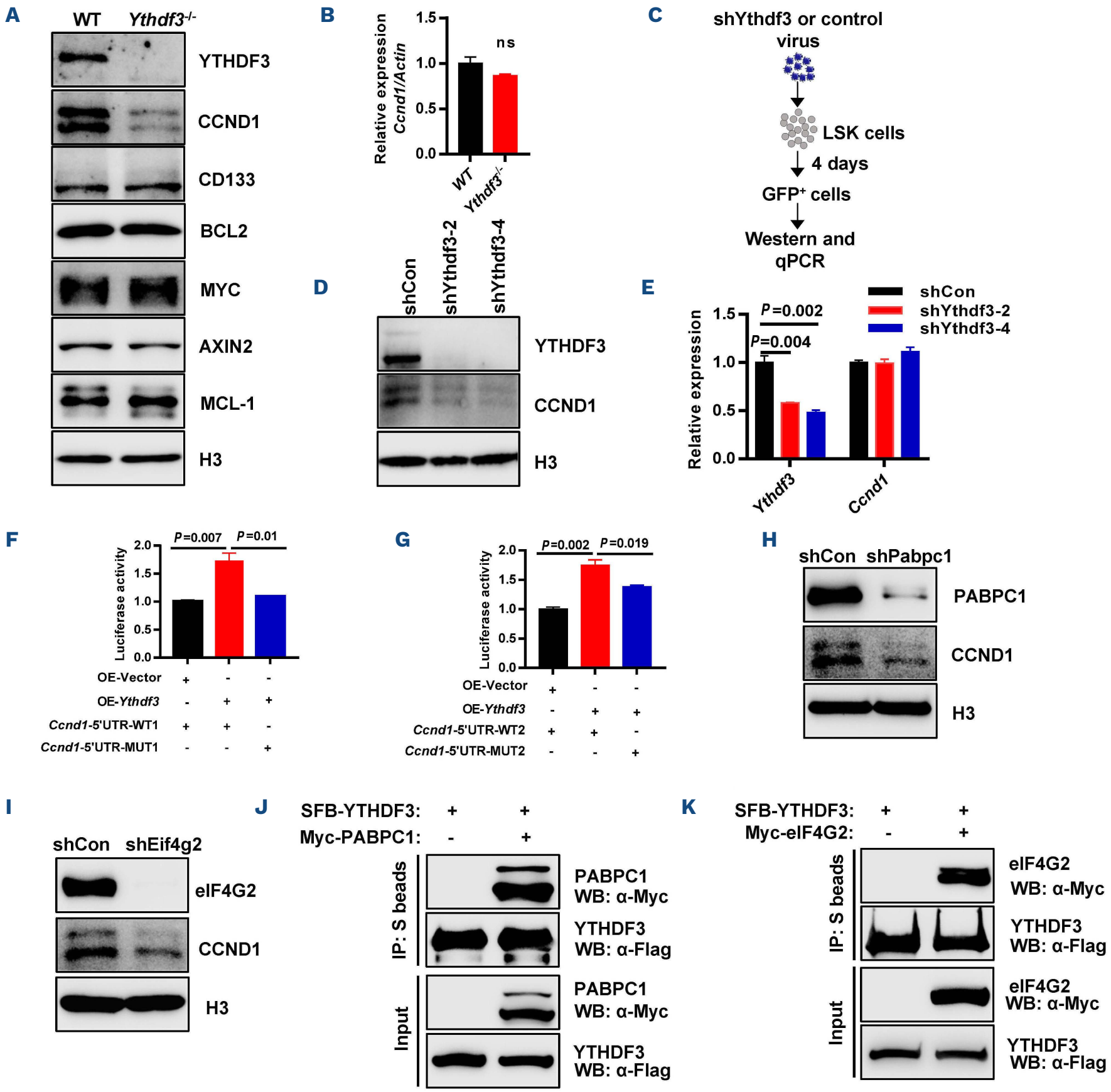

Figure 3. YTHDF3 promotes the translation of CCND1 through binding on the m^{6}A site of the 5' untranslated region. (A) Representative western blot showing the expression of YTHDF3, CCND1, CD133, BCL2, MYC, AXIN2 and MCL-1 in wildtype (WT) and *Ythdf3*$^{-/-}$ LSK cells. Freshly isolated LSK cells from WT and *Ythdf3*$^{-/-}$ mice were lysed in sodium dodecylsulfate loading buffer. Western blot analysis was performed with the indicated antibodies. (B) Histogram depicting the mRNA expression of *Ccnd1* in WT and *Ythdf3*$^{-/-}$ LSK cells. (C-E) Freshly isolated LSK cells were infected by lentivirus carrying *Ythdf3* shRNA or control, and 4 days later, GFP$^+$ cells were purified for western blot (5×10^4 cells/well) and quantitative polymerase chain reaction (qPCR) (10^5 cells) to evaluate the expression of *Ccnd1*. (C) Diagram showing the experimental design to evaluate the expression of *Ccnd1*. (D) Representative western blot showing the expression of YTHDF3 and CCND1. (E) Histogram depicting the mRNA expression of *Ythdf3* and *Ccnd1*. Data are shown as mean ± standard error of mean (SEM). (F, G) Histograms showing the relative luciferase activity of *Ccnd1*-5'UTR-WT1 or *Ccnd1*-5'UTR-Mut1 (F) and *Ccnd1*-5'UTR-WT2 or *Ccnd1*-5'UTR-Mut2 (G) luciferase reporter in 293T cells transfected with control or YTHDF3 plasmid (see *Online Supplementary Figure S3C* and *Methods*). Firefly luciferase activity was measured and normalized to Renilla luciferase activity. Data are shown as mean ± SEM. (H, I) Freshly isolated LSK cells were infected by lentivirus carrying *Pabpc1* shRNA, *eIF4G2* shRNA or control, and 4 days later, GFP$^+$ cells were purified for western blot to evaluate the expression of *Ccnd1*. Representative western blot showing the expression of PABPC1 and CCND1 (H), and eIF4G2 and CCND1 (I). (J, K) HEK293T cells were co-transfected with S-protein, Flag, and streptavidin-binding peptide (SFB)-tagged-YTHDF3 and MYC-PABPC1 or MYC-eIF4G2 plasmids for 24 h. Cell lysates were immunoprecipitated with S beads, and western blot analysis was performed with the indicated antibodies. The results show that YTHDF3 interacts with PABPC1 (J) and eIF4G2 (K). qPCR: quantitative polymerase chain reaction; IP: immunoprecipitation; WB: western blot.

four putative DRACH motifs in which m^{6}A occurs preferably: two are located at the 5'UTR and two are located at the 3'UTR of *Ccnd1* (*Online Supplementary Figure S4B*). It is notable that the first putative m^{6}A motif (-180 to -184, GGATC) is completely conserved among mice, rats and humans, while the second putative one (-102 to -106, AGACT) is only conserved between mice and humans (*Online Supplementary Figure S4C*). However, the two putative ones (GGACT) at the 3'UTR of *Ccnd1* are not conserved (*Online Supplementary Figure S4C*). This indicates that an m^{6}A motif at the 5'UTR of *Ccnd1* might play an important role in regulating *Ccnd1* mRNA translation.

We then cloned the 3'UTR of *Ccnd1* into psiCHECK2 vector (*Online Supplementary Figure S4D*) and conducted a luciferase reporter assay. The results revealed that overexpression of *Ythdf3* promotes the translation of luciferase reporters with both motifs (*Online Supplementary Figure S4F-H*). We then mutated the A at positions 1631 and 1532 to G, which is the key site of the m^{6}A motif. We observed that the translation of luciferase reporter remained unchanged (*Online Supplementary Figure S4G, H*), suggesting that these two m^{6}A motifs are not the direct region where m^{6}A modification occurs.

We next cloned the 5'UTR of *Ccnd1* containing the aforementioned DRACH motif into pGL3-Basic vector (*Online Supplementary Figure S4E*), and performed luciferase reporter assays. The results revealed that overexpression of *Ythdf3* promoted the translation of luciferase activity with both m^{6}A motifs (-180 to -184 and -102 to -106) (Figure 3F, G). We then mutated the A at positions -182 and -104 to G, and observed that luciferase activity was significantly decreased in both situations, wherein the A (-182) G mutation completely abolished the luciferase activity, while the A (-104) G mutation slightly reduced luciferase activity (Figure 3F, G).

A previous study indicated that two residues of YTHDF3, W438 and W492, contribute to the specific recognition of m^{6}A modification.[29] We therefore mutated the W438 and W492 to A (alanine) to generate a YTHDF3 mutant (YTHDF3-Mut), and overexpressed YTHDF3-WT and YTHDF3-Mut plasmids in 3T3 cells. RNA immunoprecipitation (RIP) quantitative polymerase chain reaction (qPCR for Ccnd1 revealed that YTHDF3 could bind to Ccnd1 mRNA (*Online Supplementary Figure S4I*).

These results suggest that YTHDF3 regulates the translation of CCND1 by directly binding to the 5 'UTR of *Ccnd1*, in which the -180 to -184 region is essential.

YTHDF3 promotes the translation of CCND1 by cooperating with PABPC1 and EIF4G2

Two previous studies showed that *Ythdf3* plays a critical role in translating m^{6}A-modified mRNA.[11,15] We observed that *Ythdf3* deficiency resulted in a significant decrease of protein synthesis in hematopoietic stem and progenitor cells (*Online Supplementary Figure S3E*). A previous study revealed that YTHDF3 interacts directly with the translation factor PABPC1 and eIF4G2 to promote protein translation.[29] We then explored whether YTHDF3 promotes the translation of CCND1 by interacting with PABPC1 and eIF4G2. We generated two efficient shRNA against *Pabpc1* and *Eif4g2* separately (*Online Supplementary Figure S4J, K*). We infected WT LSK cells with lentivirus carrying shRNA against *Pabpc1* and *Eif4g2* to evaluate the expression of CCND1. The results showed that knockdown of PABPC1 and eIF4G2 significantly reduced the protein level of CCND1 (Figure 3H, I).

To explore whether YTHDF3 interacted directly with PABPC1 and eIF4G2, co-immunoprecipitation was performed using anti-Flag or Myc antibody in HEK293T cells, which showed that YTHDF3 interacts directly with PABPC1 and eIF4G2 (Figure 3J, K). In addition, using RIP-qPCR assays, we found that PABPC1 and eIF4G2 bind directly with the mRNA of Ccnd1 (*Online Supplementary Figure S4L, M*). Together, these results suggest that YTHDF3 promotes the translation of CCND1 by cooperating with PABPC1 and eIF4G2.

Ccnd1 is indispensable for maintaining hematopoietic stem cells

The above data indicate that *Ccnd1* is the target of YTHDF3 to transmit the m^{6}A signal. To investigate whether *Ccnd1* plays a role in regulating HSC function, we generated two efficient guide RNA (gRNA) against Ccnd1 and cloned them (gRNA 2 and 3) (Figure 4A) into a self-made lentiviral vector (mCherry-labeled) (*Online Supplementary Figure S5A*). *Cas9*$^{flox/flox}$ GFP mice[30] were crossed with Vav1-cre to generate mice expressing CAS9 in the blood system: *Cas9*$^{flox/flox}$; *Vav1*-Cre mice (hereafter named *Cas9*$^{+/+}$ mice). Freshly isolated LSK cells of *Cas9*$^{+/+}$ mice were infected by *Ccnd1* gRNA-carrying lentivirus and 72 h later, 10,000 GFP$^+$ mCherry$^+$ cells were purified and transplanted into lethally irradiated recipients together with 2.5×10^5 competitor cells (*Online Supplementary Figure S5B*). It was found that knockdown of Ccnd1 severely impaired the reconstitution capacity of HSC (Figure 4B and *Online Supplementary Figure S5D*), which recapitulates the phenotype of *Mettl3*$^{-/-}$[16-17] and *Ythdf3*$^{-/-}$ HSC (Figure 2C).

Forced *Ccnd1* expression rescues the reconstitution capacity of *Ythdf3*$^{-/-}$ hematopoietic stem cells

Given that our data revealed that *Ccnd1* is the hub of YTHDF3 to transmit the m^{6}A signal in order to regulate its translation, and that knockdown of *Ccnd1* impaired HSC, we wondered whether forced *Ccnd1* expression could rescue the functional defect of *Ythdf3*$^{-/-}$ HSC. We, therefore, cloned Ccnd1 complementary DNA into a lentiviral vector (GFP-labeled), producing efficient overexpression of CCND1 (*Online Supplementary Figure S5C*). *Ythdf3*$^{-/-}$ LSK cells were

infected with *Ccnd1*-overexpressing lentivirus, and 3,000 CD48$^-$ Sca1$^+$ GFP$^+$ cells were FACS-purified 72 h after infection. These cells were then transplanted into lethally irradiated recipients together with 3×10^5 competitor cells (Figure 4C). The results showed that enforced *Ccnd1* expression rescued the reconstitution capacity of *Ythdf3*$^{-/-}$ HSC, including B, T and myeloid cells (Figure 4D and *Online Supplementary Figure S5E*).

To further verify this finding, we simultaneously infected freshly isolated WT LSK cells with *Ythdf3* shRNA-carrying lentivirus (GFP-labeled) and *Ccnd1*-overexpressing lentivirus (mCherry-labeled); 2,000 CD48$^-$ Sca1$^+$ GFP$^+$ mCherry$^+$

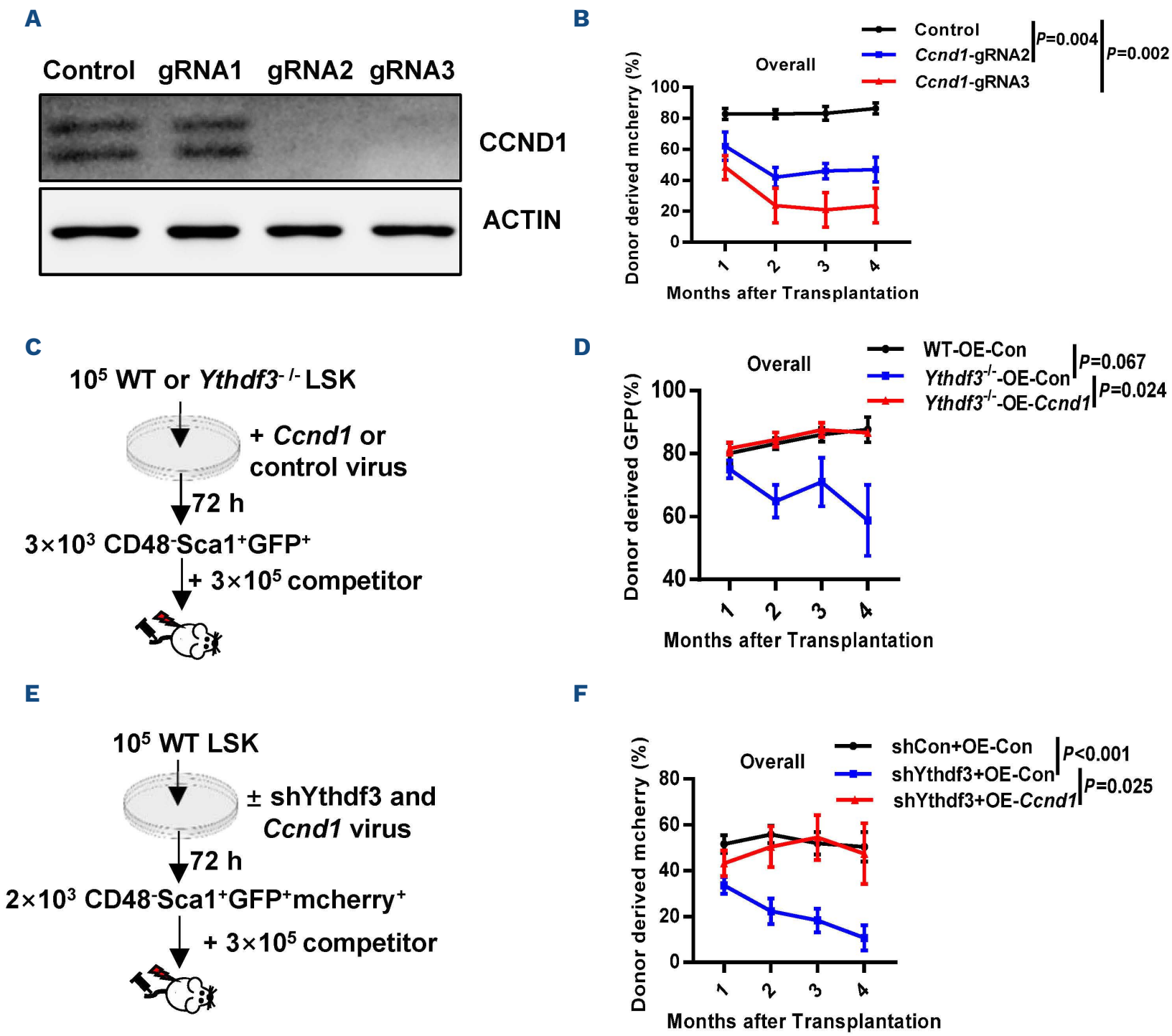

Figure 4. Overexpression of CCND1 rescues the reconstitution capacity of *Ythdf3*$^{-/-}$ hematopoietic stem cells. (A) 3T3 cells were infected by lentivirus carrying *Ccnd1* gRNA or control (GFP-labeled) and *Cas9* virus (mCherry-labeled), and 6 days later, 10^5 GFP$^+$ mCherry$^+$ cells were purified for western blot to evaluate the expression of CCND1. (B) Freshly isolated LSK cells of *Cas9*$^{+/+}$ mice were infected by *Ccnd1* gRNA-carrying lentivirus, and 72 h later, 10,000 GFP$^+$ mCherry$^+$ cells were purified and transplanted into lethally irradiated recipients together with 2.5×10^5 competitor cells. Engraftment of donor-derived cells was determined in overall (mCherry$^+$) cells every month after transplantation. Three or four mice per group. Data are shown as mean ± standard error of mean (SEM). (C, D) Freshly isolated LSK cells from wildtype (WT) or *Ythdf3*$^{-/-}$ mice were infected with *Ccnd1*-overexpressing or control virus (GFP-labeled), and 3,000 CD48$^-$ Sca1$^+$ GFP$^+$ cells were FACS-purified 72 h after infection. These cells were then transplanted into lethally irradiated recipients together with 3×10^5 competitor cells. (C) Experimental design to evaluate the role of CCND1 in regulating the reconstitution capacity of *Ythdf3*$^{-/-}$ hematopoietic stem cells (HSC). (D) Line plots depicting the percentages of donor-derived cells in overall (GFP$^+$) cells every month after transplantation. Five or six mice per group. Data are shown as mean ± SEM. (E, F) Freshly isolated LSK cells from WT mice were infected with *Ccnd1*-overexpressing virus (mCherry-labeled) and shYthdf3-carrying virus (GFP-labeled), and 2,000 CD48$^-$ Sca1$^+$ GFP$^+$ mCherry$^+$ cells were FACS-purified 72 h after infection. These cells were then transplanted into lethally irradiated recipients together with 3×10^5 competitor cells. (E) Experimental design to evaluate the role of CCND1 in regulating the reconstitution capacity of shYthdf3 HSC. (F) Line plots depicting the percentages of donor-derived cells in overall (mCherry$^+$) cells every month after transplantation. Six or seven mice per group. Data are shown as mean ± SEM.

cells were FACS-purified 72 h after infection and subsequently transplanted into lethally irradiated recipients together with 3×10^5 competitor cells (Figure 4E). It was found that enforced *Ccnd1* expression completely rescued the reconstitution capacity of *Ythdf3* shRNA-carrying HSC (Figure 4F and *Online Supplementary Figure S5F*), which is consistent with the aforementioned results (Figure 4D and *Online Supplementary Figure S5E*). Taken together, the

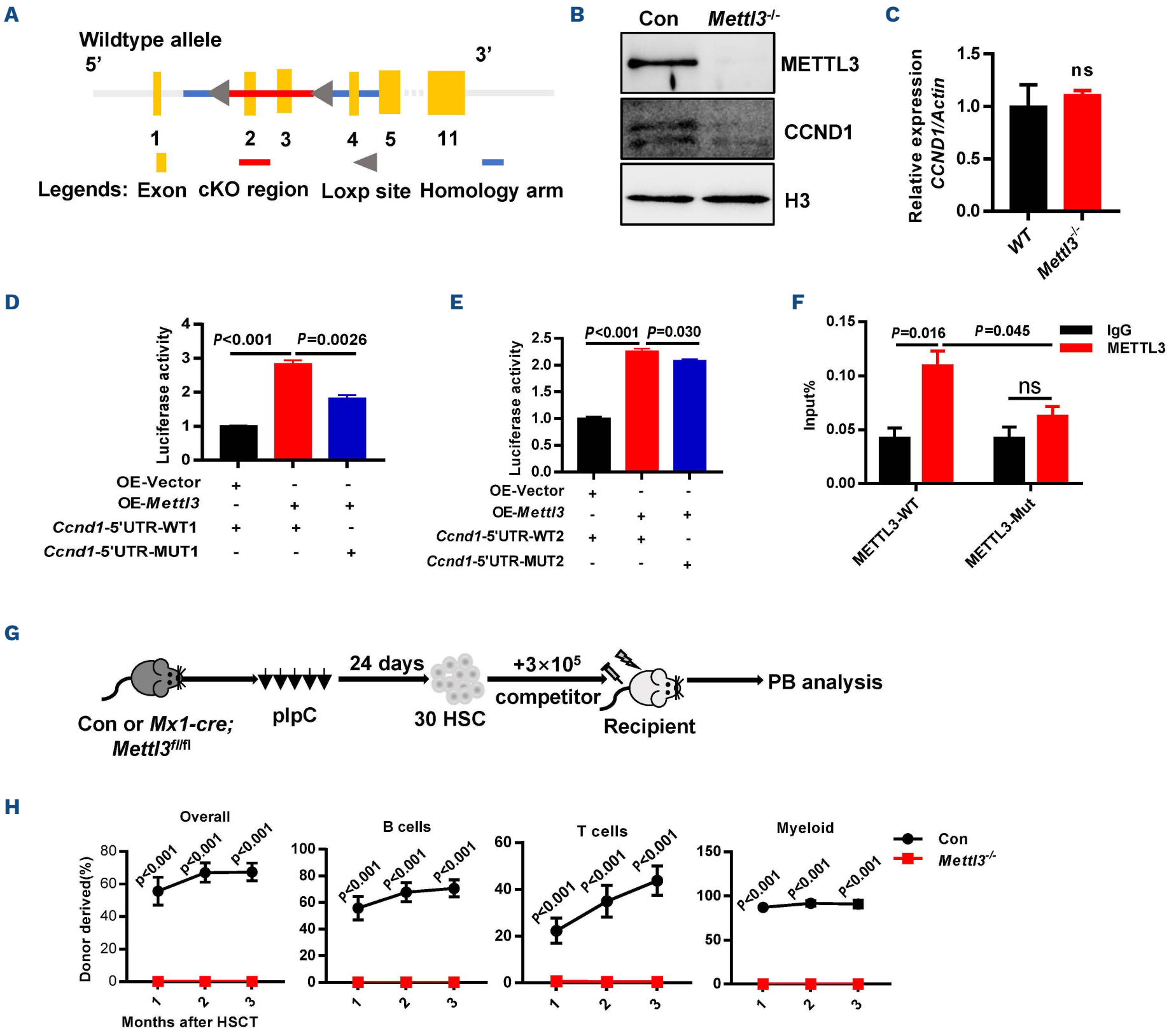

Figure 5. Dysfunction of *Mettl3* disturbs hematopoietic homeostasis and severely impairs hematopoietic stem cell reconstitution capacity. (A) Schematic illustration of the *Mettl3* conditional knockout mice. (B) Representative western blot showing the protein expression of METTL3 and CCND1 in *Mettl3*$^{-/-}$ and control LSK cells. (C) Histogram depicting the mRNA expression of *Ccnd1* in *Mettl3*$^{-/-}$ and control LSK cells. Data are shown as mean ± standard error of mean (SEM). (D, E) Histograms displaying the relative luciferase activity of *Ccnd1*-5'UTR-WT1 or *Ccnd1*-5'UTR-Mut1 (D) and *Ccnd1*-5'UTR-WT2 or *Ccnd1*-5'UTR-Mut2 (E) luciferase reporter in 293T cells transfected with control or METTL3 plasmid (see *Online Supplementary Figure S4E* and *Methods*). Firefly luciferase activity was measured and normalized to Renilla luciferase activity. Data are shown as mean ± SEM. (F) RNA immunoprecipitation quantitative polymerase chain reaction analysis detecting the binding of METTL3-WT or METTL3-Mut to the transcripts of *Ccnd1* in 3T3 cells. (G, H) Thirty freshly isolated hematopoietic stem cells from *Mettl3*$^{-/-}$ or control mice were transplanted into lethally irradiated recipients together with 3×10^5 competitor cells. Engraftment of donor cells was determined in overall (CD45.2$^+$), myeloid (Mac-1$^+$), B (B220$^+$) and T (CD3$^+$) cells every month after transplantation. (G) Scheme of the competitive transplantation strategy. (H) Line plots depicting the percentage of donor-derived cells (overall, myeloid cells, B cells, T cells) in recipients at the indicated time points. Seven mice per group. Data are shown as mean ± SEM. cKO: conditional knockout; HSC: hematopoietic stem cells; PB: peripheral blood; HSCT: hematopoietic stem cell transplantation.

above results show that *Ccnd1* is the direct target of YTHDF3 to modulate HSC reconstitution capacity.

Mettl3 modulates *Ccnd1* translation through the m^{6}A motif at the 5' untranslated region of *Ccnd1*

Given that *Ythdf3* promotes the translation of *Ccnd1* by recognizing the m^{6}A modification at the 5'UTR, we next wondered whether METTL3 installs the m^{6}A signal in the 5'UTR of *Ccnd1* and furthermore modulates the translation of *Ccnd1* through the same region. We performed a RIP-qPCR assay which showed that knockdown of *Mettl3* reduced the binding of the m^{6}A modification to *Ccnd1* transcripts (*Online Supplementary Figure S6A, B*), which revealed that METTL3 installs the m^{6}A signal on *Ccnd1* mRNA. We then generated *Mettl3*$^{flox/flox}$ mice (Figure 5A), and crossed *Mettl3*$^{flox/flox}$ with *Mx1-cre* mice to generate *Mx1-Cre*; *Mettl3*$^{flox/flox}$ mice. By administering polyinosine–polycytosine to these mice every other day for 10 days, we achieved

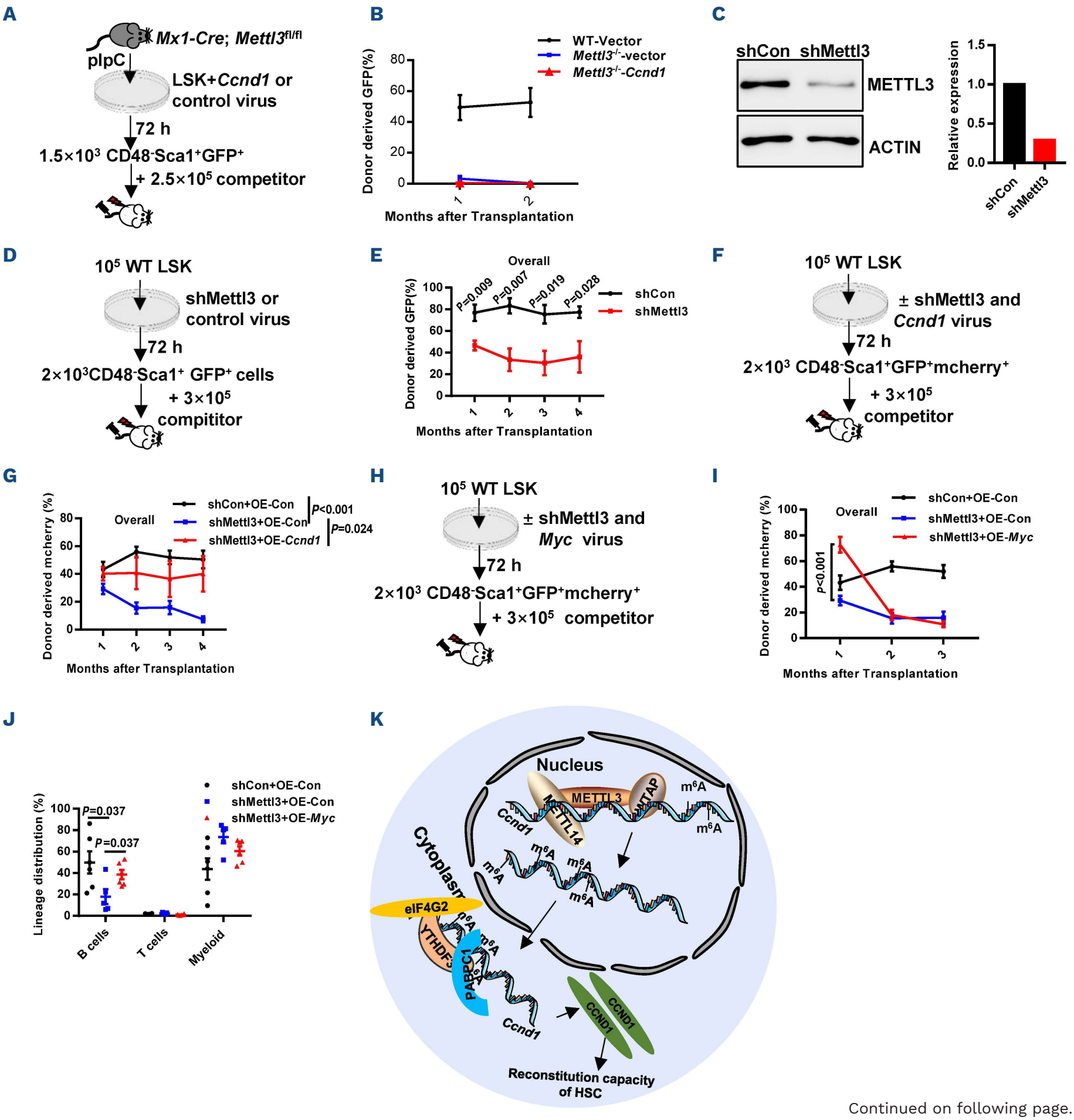

Continued on following page.

Figure 6. *Ccnd1*, but not *Myc*, is the target of METTL3 to regulate hematopoietic stem cell reconstitution capacity. (A, B) Freshly isolated LSK cells from wildtype (WT) or *Mettl3*$^{-/-}$ mice were infected with *Ccnd1*-overexpressing or control virus (GFP-labeled), and 1,500 GFP$^+$ CD48$^-$ Sca1$^+$ cells were FACS-purified 72 h after infection. These cells were then transplanted into lethally irradiated recipients together with 2.5×10^5 competitor cells. (A) Experimental design to evaluate the role of CCND1 in regulating the reconstitution capacity of *Mettl3*$^{-/-}$ hematopoietic stem cells (HSC). (B) Line plots depicting the percentage of GFP$^+$ cells in donor-derived cells every month after transplantation. Four to six mice per group. Data are shown as mean ± standard error of mean (SEM). (C) 3T3 cells were infected by lentivirus carrying *Mettl3* shRNA or control, and 4 days later, 10^5 GFP$^+$ cells were purified for western blot to evaluate the expression of METTL3: the quantitative plots are presented. (D, E) Freshly isolated WT LSK cells were infected by lentivirus carrying *Mettl3* shRNA or control and 72 h later, 2,000 CD48$^-$ Sca1$^+$ GFP$^+$ cells were purified and transplanted into lethally irradiated recipients together with 3×10^5 competitor cells. (D) Experimental design to evaluate the role of *Mettl3* in regulating the reconstitution capacity of HSC. (E) Line plots depicting the percentages of GFP$^+$ cells in donor-derived cells every month after transplantation. Five mice per group. Data are shown as mean ± SEM. (F, G) Freshly isolated LSK cells from WT mice were infected with *Ccnd1*-overexpressing virus (mCherry-labeled) and shMettl3-carrying virus (GFP-labeled), and 2,000 CD48- Sca1$^+$ GFP$^+$ mcherry$^+$ cells were FACS-purified 72 h after infection. These cells were then transplanted into lethally irradiated recipients together with 3×10^5 competitor cells. (F) Experimental design to evaluate the role of CCND1 in regulating the reconstitution capacity of *Mettl3*-compromised HSC. (G) Line plots depicting the percentage of donor-derived cells in overall (mCherry$^+$) cells every month after transplantation. (H-J) Freshly isolated LSK cells from WT mice were infected with *Myc*-overexpressing virus (mCherry-labeled) and shMettl3-carrying virus (GFP-labeled), and 2,000 CD48$^-$ Sca1$^+$ GFP$^+$ mCherry$^+$ cells were FACS-purified 72 h after infection. These cells were then transplanted into lethally irradiated recipients together with 3×10^5 competitor cells. (H) Experimental design to evaluate the role of MYC in regulating the reconstitution capacity of *Mettl3*-compromised HSC. (I) Line plots depicting the percentages of mCherry$^+$ cells in donor-derived cells every month after transplantation. (J) Scatter plot showing the lineage distribution of donor-derived mCherry^v cells in recipients at the first month. Five to seven mice per group. Data are shown as mean ± SEM. The gating strategy to generate these line plots is presented *Online Supplementary Figure S5H*. (K) This figure illustrates the proposed model of the reconstitution capacity of HSC reduced by a *Mettl3*→ RNA m^{6}A→*Ccnd1*→*Ythdf3* pathway.

total deletion of *Mettl3* in LSK cells (Figure 5B) (hereafter named *Mettl3*$^{-/-}$). Meanwhile, we investigated the mRNA and protein expression of *Ccnd1* in *Mettl3*$^{-/-}$ LSK cells and found that deficiency of *Mettl3* resulted in a significant reduction of protein level, but not of mRNA level of *Ccnd1*, in LSK cells (Figure 5B, C).

To further confirm this result, we infected WT LSK cells with lentivirus carrying shRNA against *Mettl3* to evaluate the expression of CCND1 (*Online Supplementary Figure S6C*) and found that knockdown of *Mettl3* significantly reduced the level of CCND1 protein (*Online Supplementary Figure S6D*), but not mRNA (*Online Supplementary Figure S6E*).

To further test whether *Mettl3* modulates *Ccnd1* through m^{6}A modification, we conducted a luciferase reporter assay as for *Ythdf3*. The results showed that *Mettl3* regulated the translation of *Ccnd1* through the 5'UTR region, especially the region from -180 to -184 (Figure 5D, E and *Online Supplementary Figure S6F, H*). Furthermore, based on published results, we constructed a plasmid to express the catalytic mutant METTL3 (METTL3-Mut, D395A).[9,31,32] RIP-qPCR for *Ccnd1* revealed that METTL3 could bind to *Ccnd1* mRNA (Figure 5F).

Taken together, these data suggest that METTL3 modulates the translation of *Ccnd1* by binding directly to the m^{6}A motif in the 5' UTR region.

Dysfunction of *Mettl3* disturbs hematopoietic homeostasis and severely impairs hematopoietic stem cell reconstitution capacity

To determine the influence of *Mettl3* on the production of blood cells, we performed complete blood counts of *Mettl3*$^{-/-}$ and littermate controls, which revealed that the white blood cell, lymphocyte, neutrophil, red blood cell and platelet counts were significantly decreased in *Mettl3*$^{-/-}$ mice (*Online Supplementary Figure S6I*). Meanwhile, we observed that the frequency of *Mettl3*$^{-/-}$ HSC was increased significantly compared to controls (*Online Supplementary Figure S6K*). Considering that bone marrow cellularity of *Mettl3*$^{-/-}$ mice dropped significantly (*Online Supplementary Figure S6J*), we then counted the absolute number of HSC and found that the absolute number of HSC was still increased significantly in *Mettl3*$^{-/-}$ mice (*Online Supplementary Figure S6L*), but not as dramatically as the frequency (*Online Supplementary Figure S6K*). It is notable that the expansion of HSC of *Ythdf3*$^{-/-}$ mice was much less pronounced than that of *Mettl3*$^{-/-}$ mice. The frequency of *Ythdf3*$^{-/-}$ HSC increased by 1.65 times, while the frequency of *Mettl3*$^{-/-}$ HSC increased by 82.01 times (*Online Supplementary Figure S6M*); the absolute number of *Ythdf3*$^{-/-}$ HSC increased by 1.48 times, while *Mettl3*$^{-/-}$ HSC increased by 14.51 times (*Online Supplementary Figure S6N*).

To further investigate the reconstitution capacity of *Mettl3*$^{-/-}$ HSC, 30 freshly isolated *Mettl3*$^{-/-}$ and control HSC were transplanted into lethally irradiated recipients together with 3×10^5 competitor cells (Figure 5G). The results showed that *Mettl3*$^{-/-}$ HSC failed to reconstitute the blood system (Figure 5H), which is consistent with previous reports.[16-18]

To exclude the influence of homing, 30 freshly isolated HSC from either *Mx1-Cre*; *Mettl3*$^{flox/flox}$ or control mice were transplanted into lethally irradiated recipients together with 3×10^5 competitor cells. One month after transplantation, all recipients were administered polyinosine–poly-

cytosine every other day for 10 days (*Online Supplementary Figure S7A*). It was found that deletion of *Mettl3* severely decreased the reconstitution capacity of HSC (*Online Supplementary Figure S7B1A, B*). In brief, the above results indicate that *Mettl3* is indispensable for maintaining hematopoietic homeostasis and the reconstitution capacity of HSC.

Ccnd1 is the target of METTL3 to regulate hematopoietic stem cell reconstitution capacity

Given that *Ccnd1* is the hub of METTL3 and YTHDF3 to transmit the m^{6}A signal to modulate HSC, and that forced *Ccnd1* expression rescued *Ythdf3*$^{-/-}$ HSC (Figure 4D), we then investigated whether forced *Ccnd1* expression could rescue the reconstitution capacity of *Mettl3*$^{-/-}$ HSC. We infected freshly isolated *Mettl3*$^{-/-}$ LSK cells with *Ccnd1*-overexpressing lentivirus (GFP-labeled), and 1,500 CD48$^-$ Sca1$^+$ GFP$^+$ cells were FACS-purified 72 h after infection and subsequently transplanted into lethally irradiated recipients together with 2.5×10^5 competitor cells (Figure 6A). We could not detect *Mettl3*$^{-/-}$-derived cells in the peripheral blood of recipients, while chimerism of the control group was 52.66% at the second month (Figure 6B). Thus, forced *Ccnd1* expression could not restore the reconstitution capacity of *Mettl3*$^{-/-}$ HSC.

Both previous studies[16-18] and our current results (Figure 5H and *Online Supplementary Figure S7B*) showed that *Mettl3* deficiency resulted in severe impairment of HSC, indicating that METTL3-mediated m^{6}A modification is pivotal in maintaining HSC. Chen *et al.* found that the cell function exhibited a *Mettl3* dosage-dependent effect,[33] which is an interesting observation for exploring the functional target of *Mettl3*. We, therefore, generated one shRNA against *Mettl3*, which inhibited METTL3 by 71% (Figure 6C). We then infected freshly isolated WT LSK cells with *Mettl3* shRNA-carrying lentivirus and 2,000 CD48$^-$ Sca1$^+$ GFP$^+$ were FACS-purified 72 h after infection and transplanted into lethally irradiated recipients together with 3×10^5 competitor cells (Figure 6D). The results revealed that knockdown of *Mettl3* significantly impaired the reconstitution capacity of HSC, but still retained ~36% chimerism at the fourth month (Figure 6E). This result indicates that a certain amount of METTL3 can maintain HSC function to some extent. We infected freshly isolated WT LSK cells with *Mettl3* shRNA-carrying lentivirus (GFP-labeled) and *Ccnd1*-overexpressing lentivirus (mCherry-labeled), and 2,000 CD48$^-$ Sca1$^+$ GFP$^+$ mCherry+ cells were FACS-purified 72 h after infection. These cells were then transplanted into lethally irradiated recipients together with 3×10^5 competitor cells (Figure 6F). It was found that enforced *Ccnd1* expression partially rescued the reconstitution capacity of *Mettl3* shRNA-carrying HSC (7.44±2.07 *vs.* 40.05±12.7 at the fourth month) including B, T and myeloid cells (Figure 6G and *Online Supplementary Figure S7C*).

Forced *Myc* expression cannot rescue the reconstitution capacity of *Mettl3*$^{-/-}$ hematopoietic stem cells in the long term

Previous studies showed that enforced *Myc* expression rescues the differentiation defects of *Mettl3*$^{-/-}$ HSC.[17] We therefore wondered whether forced *Myc* expression could rescue the reconstitution capacity of *Mettl3*$^{-/-}$ HSC. We infected freshly isolated *Mettl3*$^{-/-}$ LSK cells with *Myc*-overexpressing lentivirus (GFP-labeled), and 1,500 CD48$^-$ Sca1$^+$ GFP$^+$ cells were FACS-purified 72 h after infection and subsequently transplanted into lethally irradiated recipients together with 2.5×10^5 competitor cells (*Online Supplementary Figure S7D, E*). The results revealed that forced *Myc* expression could not rescue the reconstitution capacity of *Mettl3*$^{-/-}$ HSC (*Online Supplementary Figure S7F*).

To confirm this result, we infected freshly isolated WT LSK cells using *Mettl3* shRNA-carrying lentivirus (GFP-labeled) and *Myc*-overexpressing lentivirus (mCherry-labeled), and 2,000 CD48$^-$ Sca1$^+$ GFP$^+$ mCherry$^+$ cells were FACS-purified 72 h after infection. These cells were then transplanted into lethally irradiated recipients together with 3×10^5 competitor cells (Figure 6H). The results showed that overexpression of MYC significantly improved the chimera of donor-derived cells at the end of the first month (Figure 6I), and lineage analysis showed that enforced MYC expression rescued the differentiation defect of *Mettl3*-compromised HSC (Figure 6J). However, the chimera of MYC-overexpressing cells dropped rapidly in the second and third months (Figure 6I). These results suggest that overexpression of MYC did indeed rescue the differentiation defect in the first month, but was not able to rescue the reconstitution capacity of *Mettl3*-compromised HSC in the long term.

Discussion

Our study provides the first experimental evidence that the reconstitution capacity of HSC is regulated by the *Mettl3*→ *Ccnd1*→ *Ythdf3* pathway (Figure 6K). The 5'UTR of Ccnd1 is the hub for METTL3 and YTHDF3 to transmit the m^{6}A modification. This study is of great significance in revealing how a RNA m^{6}A writer and reader cooperate to modulate HSC. A more in-depth discussion is provided in the *Online Supplementary Information*.

Disclosures

No conflicts of interest to disclose.

Contribution

JW and HJ conceived the study and wrote the paper; JW, HJ, FZ and TC were responsible for the methodology; FZ, TC, LW, BZ, XW, SW, JS and ZP conducted the investigation; JW, HJ and MX performed the analyses and were re-

sponsible for the resources for this study; and JW acquired funding and supervised the study

Acknowledgments
We thank the Beijing Advanced Innovation Center for Structural Biology, the Tsinghua-Peking Center for Life Sciences and the China Telecom Corporation Limited for facilities and financial support.

Funding
This work was supported by grant numbers Z181100001818005, 81870118, 91849106, 2018YFA0800200, 2017YFA0104000 and Z200022 to JW, 61773230, 61721003, and 2020YFA0906900 to XW., and 2020YFC2008900 to PZ from the National Key R&D Program of China or the Beijing Municipal Science & Technology Commission and the National Natural Science Foundation of China.

Data-sharing statement
All raw sequencing data were deposited into the National Center for Biotechnology Information Gene Expression Omnibus with accession number GSE176458.

References

1. Morrison SJ, Scadden DT. The bone marrow niche for haematopoietic stem cells. Nature. 2014;505(7483):327-334.
2. Dzierzak E, Bigas A. Blood development: hematopoietic stem cell dependence and independence. Cell Stem Cell. 2018;22(5):639-651.
3. He H, Xu P, Zhang X, et al. Aging-induced IL27Ra signaling impairs hematopoietic stem cells. Blood. 2020;136(2):183-198.
4. Frye M, Harada BT, Behm M, He C. RNA modifications modulate gene expression during development. Science. 2018;361(6409):1346-1349.
5. Shi H, Wei J, He C. Where, when, and how: context-dependent functions of RNA methylation writers, readers, and erasers. Mol Cell. 2019;74(4):640-650.
6. Wang X, Feng J, Xue Y, et al. Structural basis of N(6)-adenosine methylation by the METTL3-METTL14 complex. Nature. 2016;534(7608):575-578.
7. Knuckles P, Lence T, Haussmann IU, et al. Zc3h13/Flacc is required for adenosine methylation by bridging the mRNA-binding factor Rbm15/Spenito to the m(6)A machinery component Wtap/Fl(2)d. Genes Dev. 2018;32(5-6):415-429.
8. Patil DP, Chen CK, Pickering BF, et al. m(6)A RNA methylation promotes XIST-mediated transcriptional repression. Nature. 2016;537(7620):369-373.
9. Wang P, Doxtader KA, Nam Y. Structural basis for cooperative function of Mettl3 and Mettl14 methyltransferases. Mol Cell. 2016;63(2):306-317.
10. Patil DP, Pickering BF, Jaffrey SR. Reading m(6)A in the transcriptome: m(6)A-binding proteins. Trends Cell Biol. 2018;28(2):113-127.
11. Shi H, Wang X, Lu Z, et al. YTHDF3 facilitates translation and decay of N(6)-methyladenosine-modified RNA. Cell Res. 2017;27(3):315-328.
12. Wang X, Lu Z, Gomez A, et al. N6-methyladenosine-dependent regulation of messenger RNA stability. Nature. 2014;505(7481):117-120.
13. Wang X, Zhao BS, Roundtree IA, et al. N(6)-methyladenosine modulates messenger RNA translation efficiency. Cell. 2015;161(6):1388-1399.
14. Du H, Zhao Y, He J, et al. YTHDF2 destabilizes m(6)A-containing RNA through direct recruitment of the CCR4-NOT deadenylase complex. Nat Commun. 2016;7:12626.
15. Li A, Chen YS, Ping XL, et al. Cytoplasmic m(6)A reader YTHDF3 promotes mRNA translation. Cell Res. 2017;27(3):444-447.
16. Yao QJ, Sang L, Lin M, et al. Mettl3-Mettl14 methyltransferase complex regulates the quiescence of adult hematopoietic stem cells. Cell Res. 2018;28(9):952-954.
17. Lee H, Bao S, Qian Y, et al. Stage-specific requirement for Mettl3-dependent m(6)A mRNA methylation during haematopoietic stem cell differentiation. Nat Cell Biol. 2019;21(6):700-709.
18. Cheng Y, Luo H, Izzo F, et al. m(6)A RNA methylation maintains hematopoietic stem cell identity and symmetric commitment. Cell Rep. 2019;28(7):1703-1716.
19. Roundtree IA, Evans ME, Pan T, He C. Dynamic RNA modifications in gene expression regulation. Cell. 2017;169(7):1187-1200.
20. Zhao BS, Roundtree IA, He C. Post-transcriptional gene regulation by mRNA modifications. Nat Rev Mol Cell Biol. 2017;18(1):31-42.
21. Deng X, Su R, Weng H, Huang H, Li Z, Chen J. RNA N(6)-methyladenosine modification in cancers: current status and perspectives. Cell Res. 2018;28(5):507-517.
22. He L, Li H, Wu A, Peng Y, Shu G, Yin G. Functions of N6-methyladenosine and its role in cancer. Mol Cancer. 2019;18(1):176.
23. Wang H, Zuo H, Liu J, et al. Loss of YTHDF2-mediated m(6)A-dependent mRNA clearance facilitates hematopoietic stem cell regeneration. Cell Res. 2018;28(10):1035-1038.
24. Li Z, Qian P, Shao W, et al. Suppression of m(6)A reader Ythdf2 promotes hematopoietic stem cell expansion. Cell Res. 2018;28(9):904-917.
25. Hendrikx PJ, Martens CM, Hagenbeek A, Keij JF, Visser JW. Homing of fluorescently labeled murine hematopoietic stem cells. Exp Hematol. 1996;24(2):129-140.
26. Bubnic SJ, Keating A. Donor stem cells home to marrow efficiently and contribute to short- and long-term hematopoiesis after low-cell-dose unconditioned bone marrow transplantation. Exp Hematol. 2002;30(6):606-611.
27. Hirayama M, Wei FY, Chujo T, et al. FTO demethylates cyclin D1 mRNA and controls cell-cycle progression. Cell Rep. 2020;31(1):107464.
28. Zhou Y, Zeng P, Li YH, Zhang Z, Cui Q. SRAMP: prediction of mammalian N6-methyladenosine (m6A) sites based on sequence-derived features. Nucleic Acids Res. 2016;44(10):e91.
29. Zhang Y, Wang X, Zhang X, et al. RNA-binding protein YTHDF3 suppresses interferon-dependent antiviral responses by promoting FOXO3 translation. Proc Natl Acad Sci U S A. 2019;116(3):976-981.
30. Platt RJ, Chen S, Zhou Y, et al. CRISPR-Cas9 knockin mice for genome editing and cancer modeling. Cell. 2014;159(2):440-455.
31. Wu R, Liu Y, Zhao Y, et al. m(6)A methylation controls pluripotency of porcine induced pluripotent stem cells by targeting SOCS3/JAK2/STAT3 pathway in a YTHDF1/YTHDF2-

orchestrated manner. Cell Death Dis. 2019;10(3):171.
32. Śledź P, Jinek M. Structural insights into the molecular mechanism of the m(6)A writer complex. Elife. 2016;5:e18434.
33. Chen WW, Qi JW, Hang Y, et al. Simvastatin is beneficial to lung cancer progression by inducing METTL3-induced m6A modification on EZH2 mRNA. Eur Rev Med Pharmacol Sci. 2020;24(8):4263-4270.
34. Xiao W, Adhikari S, Dahal U, et al. Nuclear m(6)A reader YTHDC1 regulates mRNA splicing. Mol Cell. 2016;61(4):507-519.
35. Roundtree IA, Luo GZ, Zhang Z, et al. YTHDC1 mediates nuclear export of N(6)-methyladenosine methylated mRNAs. Elife. 2017;6:e31311.
36. Hsu PJ, Zhu Y, Ma H, et al. Ythdc2 is an N(6)-methyladenosine binding protein that regulates mammalian spermatogenesis. Cell Res. 2017;27(9):1115-1127.
37. Liu J, Dou X, Chen C, et al. N(6)-methyladenosine of chromosome-associated regulatory RNA regulates chromatin state and transcription. Science. 2020;367(6477):580-586.
38. Liao S, Sun H, Xu C. YTH domain: a family of N(6)-methyladenosine (m(6)A) readers. Gen Proteomics Bioinformatics. 2018;16(2):99-107.
39. Wilson A, Murphy MJ, Oskarsson T, et al. c-Myc controls the balance between hematopoietic stem cell self-renewal and differentiation. Genes Dev. 2004;18(22):2747-2763.
40. Reavie L, Della Gatta G, Crusio K, et al. Regulation of hematopoietic stem cell differentiation by a single ubiquitin ligase-substrate complex. Nat Immunol. 2010;11(3):207-215.
41. Meyer KD, Patil DP, Zhou J, et al. 5' UTR m(6)A promotes Cap-independent translation. Cell. 2015;163(4):999-1010.
42. Chaves-Ferreira M, Krenn G, Vasseur F, et al. The cyclin D1 carboxyl regulatory domain controls the division and differentiation of hematopoietic cells. Biol Direct. 2016;11:21.
43. Choi YJ, Saez B, Anders L, et al. D-cyclins repress apoptosis in hematopoietic cells by controlling death receptor Fas and its ligand FasL. Dev Cell. 2014;30(3):255-267.
44. Kim D, Paggi JM, Park C, Bennett C, Salzberg SL. Graph-based genome alignment and genotyping with HISAT2 and HISAT-genotype. Nat Biotechnol. 2019;37(8):907-915.
45. Anders S, Pyl PT, Huber W. HTSeq--a Python framework to work with high-throughput sequencing data. Bioinformatics. 2015;31(2):166-169.
46. Subramanian A, Tamayo P, Mootha VK, et al. Gene set enrichment analysis: a knowledge-based approach for interpreting genome-wide expression profiles. Proc Natl Acad Sci U S A. 2005;102(43):15545-15550.
47. Rossi L, Lin KK, Boles NC, et al. Less is more: unveiling the functional core of hematopoietic stem cells through knockout mice. Cell Stem Cell. 2012;11(3):302-317.